

# Analysis of Tubular Structures in Medical Imaging

Jin-Woo Kim, *Member, KIMICS*

**Abstract**—A method fully utilizing multiscale line filter responses is presented to estimate the point spread function (PSF) of a CT scanner and diameters of small tubular structures based on the PSF. The estimation problem is formulated as a least square fitting of a sequence of multiscale responses obtained at each medical axis point to the precomputed multiscale response curve for the ideal line model. The method was validated through phantom experiments and demonstrated to accurately measure small-diameter structures which are significantly overestimated by conventional methods based on the full width half maximum (FWHM) and zero-crossing edge detection.

**Index Terms**—Tubular structure, Microvessel, CT, Multiscale analysis.

## I. INTRODUCTION

DIAMETER measurement of tubular structures in 3D medical data is an essential tool for quantitative evaluations of blood vessels, bronchial airways, and other similar anatomical structures. A typical method is to extract medical axes of the structures and then quantitate the width of the contour of cross-section orthogonal to the axis [1][2]. There are inherent limits on the accuracy of diameter measurement due to finite resolution of imaging scanners [3] and blurring involved in edge detectors. The influences of these limits are also discussed on thickness measurement of thin sheet structures [4][5]. In order to overcome these limits, Reinhardt et al. [6] incorporated the effects of the point spread function (PSF) of an imaging scanner

into a measurement procedure for two diameters of the cross-sectional pattern specific to bronchial airways based on model fitting of one-dimensional original intensity profiles. Its main drawbacks, however, are as follows.

- The PSF width is assumed to be known.
- The direct use of the original intensity profiles is sensitive to noise.

In this paper, we propose a method for measurement of small-diameter tubular structures based on model fitting of multiscale Gaussian blurred second derivatives along intensity ridges. The proposed method has the following advantages.

- The PSF width is estimated in the method, and thus any pre-calibration process is unnecessary.
- The use of Gaussian blurred responses along intensity ridges is expected to be relatively insensitive to noise.
- Scale-dependent constraints can be incorporated into a measurement procedure so as to improve the measurement accuracy and stability.

In our current formulation, it is assumed that 3D data sets are acquired from a CT scanner whose PSF is approximated by an isotropic Gaussian function and the cross section of tubular structure is approximated by a pill-box function (although either of these assumptions can be potentially removed). We compare the proposed method with the full width half maximum (FWHM) measure and diameter measurement based on zero-crossing contours of cross-sections.

## II. METHOD

### A. Modeling Multiscale Line Filter Response of Ideal 3D Line

A 3D tubular structure (line) orthogonal to the  $xy$ -plane is modeled as

$$Line(x; D) = Pill - Box(x, y; D) \quad (1)$$

Manuscript received November 5, 2009 ; revised December 1, 2009.

Jin-Woo Kim is with the Department of Multimedia and Communication Engineering, Kyungsoo University, Busan, 314-79, Korea (Tel: +82-51-663-5153, Fax: +82-51-625-1402, Email: jinwoo@ks.ac.kr)

Where  $x = (x, y, z)^T$ ,  $D$  is the line diameter, and

$$Pill - Box(x, y; D) = \begin{cases} 1 & \sqrt{x^2 + y^2} < \frac{D}{2} \\ 0 & \sqrt{x^2 + y^2} > \frac{D}{2} \end{cases} \quad (2)$$

Here, line structures are assumed to be brighter than surrounding regions.

The point spread function (PSF) of a CT scanner is assumed to be described by  $Gauss(x; \sigma_{psf})$ , where  $Gauss(x; \sigma)$  is the isotropic 3D Gaussian function, and  $\sigma_{psf}$  denotes the PSF width. The intensity function of 3D data  $f_{line}(x; D, \sigma_{psf})$ , of line diameter  $D$  imaged by a CT scanner of PSF width  $\sigma_{psf}$  is given by

$$f_{line}(x; D, \sigma_{psf}) = Line(x; D) * Gauss(x; \sigma_{psf}) \quad (3)$$

where  $*$  denotes the convolution operation.

When the Gaussian filters are applied to the acquired 3D data by postprocessing, the Gaussian filtered 3D data of a line are described by

$$f_{line}(x; D, \sigma_{psf}, \sigma_f) = Line(x; D) * Gauss(x; \sigma_{psf}) * Gauss(x; \sigma_f) \quad (4)$$

where  $\sigma_f$  is the filter width. The Gaussian filtered line with intensity height  $H$  is described by  $H \cdot f_{line}(x; D, \sigma_{psf}, \sigma_f)$ . In our problem,  $D$ ,  $H$ , and  $\sigma_{psf}$  are unknown and need to be estimated from 3D data while  $\sigma_f$  is known.

In the proposed approach, we fully utilize the scale-dependency of the line filter responses in order to estimate line diameter  $D$  as well as PSF width  $\sigma_{psf}$  and line height  $H$ . We consider the line filter responses,  $R(\sigma; D)$ , of the ideal 3D line at the line axis, that is,  $x=(0,0,z)$ , which is given by

$$R(\sigma; D) = \sigma^2 \cdot \frac{\partial^2}{\partial x^2} f_{line}(0,0,z; D, \sigma_{psf}, \sigma_f) \quad (5)$$

where  $\sigma = \sqrt{\sigma_{psf}^2 + \sigma_f^2}$ , and  $\sigma^2$  is multiplied for scale-normalization of the responses. Given  $D$ ,

$\sigma_{psf}$ ,  $R(\sigma; D)$  can be calculated using Eq. (5). Fig.1 shows an example of  $R(\sigma; D)$  calculated numerical simulation.

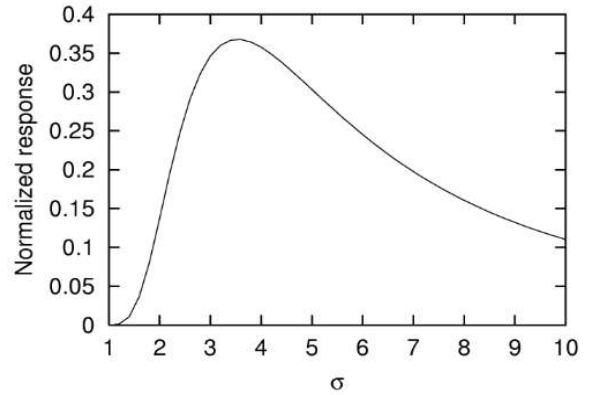


Fig. 1 Normalized line filter responses,  $R(\sigma; D)$ , of ideal 3D line at line axis. ( $D=10$ , and  $\sigma = 0.36D$ )

### B. Extracting a Sequence of Multiscale Line Filter Responses on medial Axis from 3D Data

Let the intensity function of Gaussian filtered 3D data be  $f(x; \sigma_{psf}, \sigma_f)$  or  $f(x; \sigma)$ , where  $\sigma = \sqrt{\sigma_{psf}^2 + \sigma_f^2}$ . The gradient vector of  $f(x; \sigma)$  is defined as  $\nabla f(x; \sigma) = (f_x(x; \sigma), f_y(x; \sigma), f_z(x; \sigma))^T$ , where partial derivatives of  $f(x; \sigma)$  are represented as  $f_x(x; \sigma) = \partial/\partial x f(x; \sigma)$ , and so on. The Hessian matrix of  $f(x; \sigma)$  is given by

$$\nabla^2 f(x; \sigma) = \begin{bmatrix} f_{xx}(x; \sigma) & f_{xy}(x; \sigma) & f_{xz}(x; \sigma) \\ f_{yx}(x; \sigma) & f_{yy}(x; \sigma) & f_{yz}(x; \sigma) \\ f_{zx}(x; \sigma) & f_{zy}(x; \sigma) & f_{zz}(x; \sigma) \end{bmatrix}$$

where  $f(x; \sigma)$  are represented as  $f_{xx}(x; \sigma) = \partial^2/x^2 f(x; \sigma)$ ,  $f_{yz}(x; \sigma) = \partial^2/\partial y \partial z f(x; \sigma)$ , and so on.

Let the eigenvalues of  $\nabla^2 f(x; \sigma)$  be  $\lambda_1, \lambda_2, \lambda_3$  ( $\lambda_1 \geq \lambda_2 \geq \lambda_3$ ) and their corresponding eigenvectors be  $e_1, e_2, e_3$  ( $|e_1| = |e_2| = |e_3| = 1$ ), respectively.  $e_1$  is expected to give the tangential direction of the line and the line filter response is obtained as the combination of  $\lambda_2$  and  $\lambda_3$ , directional second derivatives orthogonal to  $e_1$ .

We assume that the tangential direction of line is given by  $e_1$  at the voxel around the medial axis. The 2D intensity function,  $c(u)$  ( $u = (u, v)^T$ ), on the

cross-sectional plane of  $f(x; \sigma)$  orthogonal to  $e_1$ , should have its peak on the medial axis. The second-order local approximation of  $c(u)$  is given by

$$c(u) = f(x_0; \sigma) + u^T \nabla c_0 + \frac{1}{2} u^T \nabla^2 c_0 u \quad (6)$$

where  $ue_2 + ve_3 = x - x_0$ ,  $\nabla c_0 = (\nabla f \cdot e_2, \nabla f \cdot e_3)^T$  ( $\nabla f$  is the gradient vector, that is,  $\nabla f(x_0; \sigma)$ ), and

$$\nabla^2 c_0 = \begin{bmatrix} \lambda_2 & 0 \\ 0 & \lambda_3 \end{bmatrix}$$

$c(u)$  should have its peak on the medial axis of the line. The peak is located at the position satisfying

$$\frac{\partial}{\partial u} c(u) = 0 \quad \text{and} \quad \frac{\partial}{\partial v} c(u) = 0 \quad (7)$$

By solving Eq. (7), we have the offset vector,  $p = (p_x, p_y, p_z)^T$ , of peak position from  $x_0$  given by  $p = se_2 + te_3$ , where  $s = -(\nabla f \cdot e_2 / \lambda_2)$  and  $t = -(\nabla f \cdot e_3 / \lambda_3)$ . For the medial axis to exist at the voxel  $x_0$ , the peak of  $c(u)$  needs to be located in the territory of voxel  $x_0$ . Thus, the medial axis element, that is, medial axel, is detected only if  $|p_x| \leq 0.5$  &  $|p_y| \leq 0.5$  &  $|p_z| \leq 0.5$  (voxels). By combining the voxel position  $x_0$  and offset vector  $p$ , the medial axel is localized at subvoxel resolution.

We define the line filter response as  $\sigma_f^2 \sqrt{\lambda_2 \lambda_3}$  in this paper, where  $\sigma_f^2$  is multiplied to normalize the responses. A sequence of multiscale line filter responses,  $R_i$ , of different filter widths  $\sigma_{f_i}$  ( $i = 1, 2, 3, \dots$ ) is extracted at each detected medial axel as follows.

1. The medial axel detection and line filtering are performed at different scales  $\sigma_{f_i}$  ( $i = 1, 2, 3, \dots$ ).
2. The medial axel having the strongest line filter response is selected among all the detected axels irrespective to scales. Let the strongest axel be found at  $x_0$  of  $\sigma_{f_{i_0}}$ .
3. The axels nearest and within one-voxel distance to position  $x_0$  are extracted at adjacent scales  $\sigma_{f_{i_0+1}}$  and  $\sigma_{f_{i_0-1}}$ . Similarly, the axels are extracted in larger and smaller scales until no axels are found.

### C. Estimation Processes

The basic strategy is to find  $D$ ,  $H$ , and  $\sigma_{psf}$  minimizing the square sum of differences between the model  $H \cdot R(\sigma; D)$  and the data set at each axel, that is, a sequence of multiscale line filter responses,  $R_i$ , of different filter widths  $\sigma_{f_i}$  ( $i = i_s, \dots, i_e$ ) where  $i_s$  and  $i_e$  are the smallest and largest scales, respectively, in the sequence at the axel of interest.

The estimation processes consist of two stages. During the first stage,  $\sigma_{psf}$  and  $H$  are estimated using the axels which have relatively large diameters and whose positions are close to the voxel center. During the second stage,  $D$  is estimated for every sequence of multiscale filter responses using  $\sigma_{psf}$  and  $H$  estimated in the first stage.

#### 1) Estimating PSF of CT imaging and intensity height of line

To accurately estimate PSF width  $\sigma_{psf}$  and intensity height  $H$ ,  $R_i$  needs to be fit to the model  $R(\sigma; D)$  in a wide range of scale  $\sigma$  including the range around maximum values of  $R(\sigma; D)$ . Furthermore, the axel position localized in subvoxel accuracy should be close to the voxel center to guarantee the response is the peak response or close to it. We selected the sequences satisfying the following conditions.

1.  $i_t < \arg \max_i R_i$ , where  $\sigma_{f_{i_t}}$  should be sufficiently large.
2.  $\sqrt{|p_x|^2 + |p_y|^2 + |p_z|^2} < d_t$ , where  $d_t$  is a constant representing the maximum distance to the voxel center to be allowed. In the experiment, we used  $d_t = 0.3$  (voxels).

For the sequences of multiscale filter responses satisfying the above conditions,  $\sigma_{psf}$ ,  $D$ , and  $H$  are searched which minimize

$$E_1(\sigma_{psf}, H, D) = \sum_{i=i_s}^{i_e} \left\{ H \cdot R(\sqrt{\sigma_{psf}^2 + \sigma_{f_i}^2}; D) - \frac{\sigma_{psf}^2 + \sigma_{f_i}^2}{\sigma_{f_i}^2} R_i \right\}^2 \quad (8)$$

where  $i_s$  and  $i_e$  are the smallest and largest scales in the extracted sequence of multiscale filter responses at the axel of interest.

In the experiments, exhaustive search was applied

to  $D$  and  $\sigma_{psf}$ .  $D$  was discretized from 0.02 to 24.0 voxels with 0.02 voxel interval, and  $\sigma_{psf}$  was discretized from 0.02 to 4.0 voxel with 0.02 voxel interval. For all the combinations of discretized  $D$  and  $\sigma_{psf}$ ,  $H$  was estimated by minimizing Eq. (8). With known  $D$  and  $\sigma_{psf}$ , the estimation of  $H$  minimizing Eq. (8) is formulated as a linear square problem. Thus,  $D$ ,  $\sigma_{psf}$ , and  $H$  are obtained for each sequence of multiscale responses. We assume that  $\sigma_{psf}$  and  $H$  are not locally variable.  $\sigma_{psf}$  and  $H$  are obtained as averages of all the results from the sequences of multiscale responses considered at this stage.

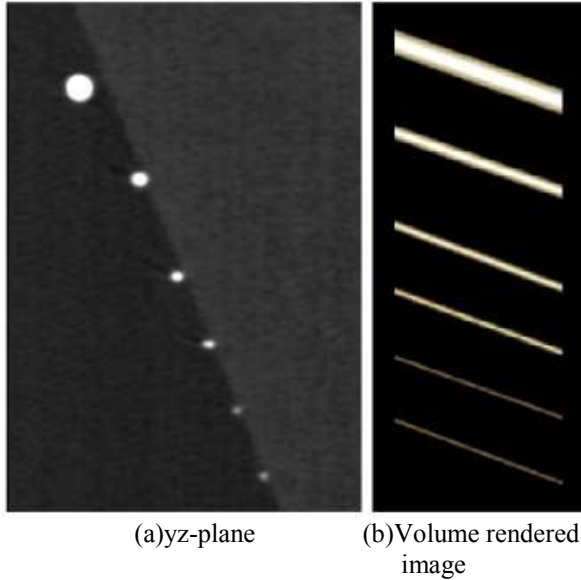


Fig. 2 CT volume data of several diameters of acrylic rods.

### 2) Diameter estimation

For all the extracted sequences of multiscale filter responses, using known  $H$  and  $\sigma_{psf}$ ,  $D$  is searched minimizing

$$E_2(D) = \sum_{i=i_s}^{i_t} \left\{ H \cdot R(\sigma; D) - \frac{\sigma^2}{\sigma_{f_i}^2} R_i \right\}^2 \quad (9)$$

where  $\sigma = \sqrt{\sigma_{psf}^2 + \sigma_{f_i}^2}$ . In the experiments, exhaustive search was applied to  $D$ .  $D$  was discretized from 0.02 to 24.0 voxels with 0.02 voxel interval.

## III. EXPERIMENTAL RESULTS

CT volume data of several diameters of acrylic rods were acquired using CT scanner. Isotropic voxel imaging was performed with voxel size of  $0.5 \text{ mm}^3$ . The diameters of acrylic rods were 3.0, 1.6, 1.0, 0.75, and  $0.5 \text{ mm}$ . A cross-sectional image in the  $yz$ -plane of the acquired CT data and its volume rendered image are shown in Fig. 2. The rods were straight and the angle of their axes was approximately 20 degrees to the  $xy$ -plane of the CT coordinate system. The volume data were trimmed and sinc-interpolated so that the voxel interval was  $0.25 \text{ mm}$ . The multiscale filter widths were  $\sigma_{f_i} = 2^{i-1/4}$  (voxels), where  $i=1, 2, 3, \dots, 11$  (the voxel size is  $0.25 \text{ mm}^3$ ).

The estimation results in the first stage were  $\sigma_{psf}=1.61(\text{voxels}) = 0.40(\text{mm})$  and  $H=1054$ , where the voxel size that of the interpolated volume data, that is,  $0.25 \text{ mm}^3$ . Fig. 3 shows the results of diameter estimation at the second stage. The averages and standard deviations of the experimentally estimated diameters of five rods are indicated in Fig. 3.

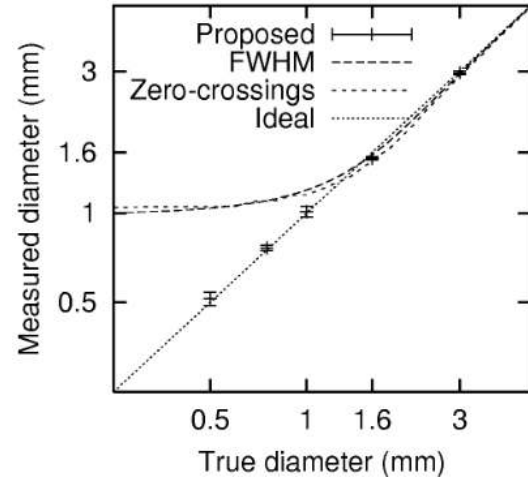


Fig. 3 Results of diameter measurement.

Since the results of the proposed method were experimentally measured, the averages and standard deviations for diameters 3.0, 1.6, 1.0, 0.75, and  $0.5 \text{ mm}$  are indicated as errorbars. The ideal relation was plotted as a dotted line. Fig. 3 also shows simulation results of the diameters estimated using full width half maximum (FWHM) and using zero-crossings of radial directional second derivatives orthogonal to medial axis. These results are plotted as

dashed lines since they are numerically computed. In the simulations,  $\sigma_{psf} = 0.40(mm)$  was used. In the simulations of zero-crossings, computation of second derivatives was assumed to be combined with Gaussian blurring of standard deviation of 1.2(voxels) = 0.3(mm). In diameter estimations using FWHM and zero-crossings, significant overestimation was observed when the actual diameter was 1.0 mm or less. In the proposed diameter estimation, accurate measurement was realized even for diameters 1.0 mm, 0.75 mm, and 0.5 mm.

#### IV. CONCLUSIONS

We have described a method for accurate measurement of small-diameter tubular structures. This work provides a unified approach based on multiscale filter responses to the estimation of the point spread function (PSF) of a CT scanner as well as the estimation of diameters. The method is validated through phantom experiments and demonstrated to accurately measure small-diameter structures which are significantly overestimated by conventional methods based on full width half maximum (FWHM) and zero-crossing edge detection.

Because the method is based on second derivatives, it is insensitive to the DC component, that is, the background level, of image intensity. However, inaccuracy in the estimated intensity height  $H$  may affect the estimated diameter accuracy. We are planning to quantitatively evaluate this effect. Future work will also include the effects of inaccuracy in the PSF width  $\sigma_{psf}$ . In this paper, we have assumed isotropic imaging and circular cross-section of the straight tubular structures on a uniform background. The validation needs to be completed on the robustness with respect to anisotropic resolution, non-circular cross-section, the curvature of the structure, and a non-uniform background.

The proposed method is related to the heuristics that the scale at which the maximum normalized response is obtained is selected as the optimal scale of the tubular structures[7][8]. The optimal scale  $\sigma_{psf} = 0.36D$  is observed when they have pill-box shapes (as shown in Fig. 1). In this heuristics, the effect of the imaging scanner PSF is not considered. When the effect of PSF is considered, the maximum response is inherently not obtainable for small-diameter structures which do not satisfy the condition  $(1/0.36) \cdot \sigma_{psf} < D$ . Further, the output of this heuristics is discrete. In the proposed method, by least

square fitting of multiscale responses to the theoretical multiscale response curve, accurate, continuous estimates are obtained even for small-diameter structures not satisfying  $(1/0.36) \cdot \sigma_{psf} < D$ .

For clinical application, a multiscale tracking method for tubular structures in 3D data as described in [8] can be effectively combined with the proposed method. We are now developing a method for scale-space tracking of extracted axels to combine with the proposed method.

#### ACKNOWLEDGMENT

This research was supported by Kyungsoong University Research Grants in 2009(2009281).

#### REFERENCES

- [1] A. F. Frangi, W. J. Niessen, et al., "Model-based quantitation of 3D magnetic resonance angiographic," *IEEE Trans. Med. Imaging*, vol. 18, pp. 946–956, Oct. 1999.
- [2] O. Wink, W. J. Niessen, M. A. Viergever, "Fast delineation and visualization of vessels in 3D angiographic images," *IEEE Trans. Med. Imaging*, vol. 19, pp. 337–346, Apr. 2000.
- [3] R. M. Hoogeveen, C. J. Bakker, M. A. Viergever, "Limits to the accuracy of vessel diameter measurement in MR angiography," *JMRI*, vol. 8, pp. 1228–1236, 1998.
- [4] S. Prevrhal, K. Engelke, W. A. Kalender, "Accuracy limits for the determination of cortical width and density: the influence of object size and CT imaging parameters," *Phys. Med. Biol.*, vol. 44, pp. 751–764, Mar. 1999.
- [5] G. Dougherty, D. Newman, "Measurement of thickness and density of thin structures by computed tomography: simulation study," *Med. Phys.*, vol. 26, pp. 1341–1348, 1999.
- [6] J. M. Reinhardt, N. D. Souza, E. A. Hoffman, "Accurate measurement of intrathoracic airways," *IEEE Trans. Med. Imaging*, vol. 16, pp. 820–827, 1997.
- [7] K. Krissian, G. Malandain, N. Ayache, "Model-based detection of tubular structures in 3D images," *Computer Vision and Image Und.*, vol. 80, pp. 130–171, 2000.
- [8] S. R. Aylward, E. Bullitt, "Initialization, noise, singularities, and scale in height ridge traversal for tubular object centerline extraction," *IEEE Trans. Med. Imaging*, vol. 21, pp. 61–75, 2002.

**Kim, Jin Woo**

He received the B.S degree in Electrical Engineering from Myongji University in 1992 and the M.S and Ph.D. degrees in Electronic Engineering and System design Engineering from Fukui University, Fukui, Japan, in 1996 and 1999, respectively. From 2000 to 2003, he was a contract Professor in the Department of Information Communication and Computer Engineering at Hanbat National University, Daejeon, Korea. Since 2003 he has been with the Department of Multimedia and Communication Engineering at Kyungsoong University, Busan, Korea, where he is currently an associate professor. From Dec., 2007 to Mar., 2009, he was a visiting researcher in the Department of Bioengineering at Tokyo University, Japan. His current research interests include image processing, pattern recognition, and medical imaging technology.